

# Vibrational and Translational Energy Effects in the Reaction of Ammonia Ions with Water Molecules

Michael A. Everest, John C. Poutsma, and Richard N. Zare\*

Department of Chemistry, Stanford University, Stanford, California 94305

Received: May 20, 1998; In Final Form: July 29, 1998

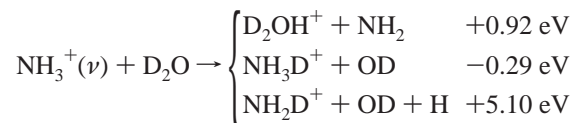
The reaction of vibrationally state-selected ammonia ions with deuterated water is investigated with a quadrupole–octopole–quadrupole apparatus. Relative integral reaction cross sections for all ionic products are measured for collisional energies from 0.5 to 10.0 eV (center of mass) and ammonia ion vibrational states  $1^0 2^{0-10}$  and  $1^1 2^2$ . The predominant charged products have masses of 18 and 21 amu and are shown to be  $\text{NH}_2\text{D}^+$  (formal isotope exchange) and  $\text{D}_2\text{OH}^+$  (proton transfer), respectively. Small amounts of product are also observed at masses 19, 20, and 22 amu. The cross section for proton transfer decreases with increasing collisional energy, but it increases with increasing internal energy at all collisional energies studied. The cross section for formal isotope exchange increases with increasing collisional energy and increases with increasing internal energy only at low collisional energies. Comparing the reactivity of  $\text{NH}_3^+(1^0 2^5)$  to that of  $\text{NH}_3^+(1^1 2^2)$  (internal energies of 0.60 and 0.63 eV, respectively) shows whether the system is sensitive to the specific vibrational motion, or only to the total amount of internal energy. The present system is shown not to be vibrational-mode selective—the two internal preparations having comparable reactive cross sections at all collisional energies studied. The projection of the product velocity onto the ion-beam axis is obtained by transforming the experimentally measured product time-of-flight profiles. These velocity profiles contain information regarding energy released into product recoil. The isotope exchange products scatter tightly (0.6 eV, hwhm) about the center of mass and display forward–backward symmetry. The proton-transfer products yield a bimodal velocity distribution with one peak in the backward direction and another on the center of mass. The data observed for the isotope-exchange product indicate a reaction mechanism in which the first step is collision-induced dissociation of the ammonia ion (or water molecule), resulting in a hydrogen (deuterium) atom and an  $[\text{NH}_2\text{D}_2\text{O}]^+$  ( $[\text{NH}_3\text{OD}]^+$ ) complex. This complex may decay to form the products  $\text{NH}_2\text{D}^+$  and OD (OH). The majority of the  $\text{D}_2\text{OH}^+$  product is formed via direct proton transfer.

## Introduction

Elaborate methods are often necessary to determine the finer details that comprise complex processes, especially if the events under consideration are not directly observable. In these difficult cases it is necessary to control precisely conditions preceding the event, as well as accurately observe many of the conditions of the system after the process has taken place. If the system under investigation is the chemical reaction of two polyatomic molecules, the conditions before the reactive encounter that may be controlled include the internal state distribution (rotational, vibrational, and electronic) of each reactant, the relative speed with which the individual reactants approach each other before colliding, and the relative orientation of the reactants. The properties of the system available for observation following the reactive event include the identity of all the products (and their likelihood of formation were the experiment to be repeated many times), their internal state distributions, their relative orientation, and the velocities with which they recoil from the location of the collision. To date, there is a substantial history of this type of detailed investigation of chemical reactions.<sup>1</sup>

The present study is an investigation of the reaction of an ammonia ion ( $\text{NH}_3^+$ ) with a deuterated water molecule ( $\text{D}_2\text{O}$ ) in which the vibrational state of the ammonia ion as well as

the translational energy is experimentally controlled. After the reactive collision we measure the relative abundance of all ionic products, irrespective of scattering angle, as well as the projection of each ionic product's velocity onto an axis in the laboratory frame. These results and their implications are presented below; however, the observed channels are presented here for the sake of the present discussion. The observed channels are



(Reported values for the energies of the reactions are  $\Delta E$  at 0 K.<sup>2</sup>) Although some factors are not controlled rigorously (e.g., the internal energy of the water molecules) and many properties after the collision are not measured (internal states of the products, abundance of neutral products, etc.), we are still able to extract much information from the experimental results.

Ours is not the first study of the reaction of ammonia ions with water molecules. In 1968 Chupka and Russell<sup>3</sup> measured the efficiency of the reaction of internally excited  $\text{NH}_3^+$  with  $\text{H}_2\text{O}$  to form both  $\text{NH}_4^+$  and  $\text{H}_3\text{O}^+$ . The ammonia ions were prepared with various amounts of internal energy by means of photoionization, which was quite a feat before the advent of lasers in the chemistry laboratory! They reported a slight (10%)

\* To whom correspondence should be addressed.

enhancement of the reaction to form  $\text{NH}_4^+$  upon the addition of  $\approx 1.5$  eV of internal energy in the ammonia ion. Formation of  $\text{H}_3\text{O}^+$  was seen to be a factor of 100 less probable than formation of  $\text{NH}_4^+$  under their experimental conditions.

Nine years later the problem was taken up by Anicich, Kim, and Huntress.<sup>4</sup> They employed two different ICR methods to determine the product branching and rates of reaction for the reaction of internally excited  $\text{NH}_3^+$  with  $\text{H}_2\text{O}$ . They determined that ammonia ions in the ground vibrational state react with water to form only  $\text{NH}_4^+$ , whereas internally excited ammonia ions produce both  $\text{NH}_4^+$  and  $\text{H}_3\text{O}^+$  (15% and 85%, respectively). Moreover, they showed that the overall rate of reaction of internally excited ammonia ions is much faster than that of ground-state ions.

Chesnavich and Bowers<sup>5</sup> compared the results of both above-mentioned experiments with the predictions of statistical phase space theory and concluded that the reactions in question proceed nonstatistically.

Adams, Smith, and Paulson<sup>6</sup> reacted ammonia ions with water molecules at thermal collisional energies in a SIFT. As with Anicich et al., they observed only  $\text{NH}_4^+$  from this reaction under energetically thermal conditions. They found the binary rate constant for this reaction to be  $< 3 \times 10^{-11}$ —much less than the theoretical (ADO) value of  $2.38 \times 10^{-9}$ .

Kemper et al.<sup>7</sup> used their own measurements, along with those of Anicich et al.,<sup>4</sup> to probe the internal energy deposited into the ammonia ion after charge transfer from one of several molecular ions or rare gas ions. In this study they used the reaction of ammonia ions with water molecules as an indicator of the total amount of internal energy deposited in the ions by charge transfer. They first calibrated the scheme with rare gas ions as the charge carrier, using energy balance and the measured kinetic energy release to determine the amount of internal energy in the ammonia ion. Once the charge-transfer reactions are well characterized, the amount of internal (total vibrational and rotational) energy in the ammonia ions from a chemical ionization source is known, and the dependence of chemical reactions on ammonia ion internal energy can be studied for each observed channel. ( $\text{H}_3\text{O}^+$  and  $\text{NH}_4^+$  were the observed products.) The rate to form  $\text{H}_3\text{O}^+$  was seen to increase sharply at ammonia ion internal energies above 2 eV, whereas that to form  $\text{NH}_4^+$  decreased gradually over the range 1–3 eV and remained very low at higher energies. They estimated the collisional energy of the reactions to be less than 0.2 eV for these ICR measurements.

Tachibana et al.<sup>8</sup> have performed detailed density functional theory calculations on the present system as well as the reactions of ammonia ions with ammonia and hydrogen fluoride. Although they calculated the energies for many of the pertinent species discussed in the present work, their discussion dwelt mainly on the hydrogen abstraction reaction, which is nearly unobservable at high collisional energies.

More recently, Green and Zare<sup>9</sup> studied the reaction of ammonia ions with water molecules (both fully deuterated) in a bulb. They investigated the reaction of ammonia ions in both the ground and the first excited vibrational state ( $\nu_2$ ). They measured rotational distributions of OD from the reaction channel  $\text{ND}_3^+ + \text{D}_2\text{O} \rightarrow \text{ND}_4^+ + \text{OD}$  and found them to agree well with the predictions of statistical theory.

It is surprising that, although the species under investigation in this study are both common in nature and increasingly accessible to theoretical calculation, ours is the first study of this system at collisional energies significantly above thermal energies. Because we are investigating this reaction under

drastically different energetic conditions, the insight gained from comparison with past results has been limited.

Our investigation of this reaction is unique not only because of the high collisional energies involved but also because we have direct control of the internal state of the ammonia ion. This control is possible as the ions are prepared via resonant multiphoton ionization. In addition, more than one normal vibrational mode may be excited upon ionization, allowing the investigator to test the sensitivity of the reaction to the vibrational mode of the ion, not just the total internal energy. This type of mode-selective investigation has been done for both neutral/neutral and ion/neutral reactions.<sup>10</sup> Although statistical theories have seen much success in describing the behavior of ion–molecule reactions, a few cases exist where mode selectivity is observed. Past work in this laboratory on the reaction of ammonia ions with fully deuterated ammonia molecules<sup>11</sup> showed charge transfer to be enhanced for ammonia ions with energy in the “umbrella” bending mode ( $\nu_2$ ) compared to ions with energy in the symmetric stretching mode ( $\nu_1$ ). Anderson and co-workers have also seen mode-selective behavior in reactions of both state selectively prepared acetylene ions<sup>12</sup> and state selectively prepared ammonia ions.<sup>13</sup> These previous investigations of mode-selective behavior of ion–molecule reactions seem to indicate that energy in vibrational modes whose motions are along the reaction coordinate tend to enhance reactivity; however, there are also cases where excitation in a mode whose motion seems to be along the reaction coordinate does not enhance reactivity. For example, while charge transfer from ammonia ions to fully deuterated ammonia is enhanced with “umbrella” bending, the proton transfer is not significantly enhanced with the symmetric stretching motion. The reaction of ammonia ions with deuterated water is a good test case for the criteria for mode-selective behavior because it has at least two product channels but no observed charge transfer.

## Experimental Method

The experimental method employed is described more fully elsewhere;<sup>14,15</sup> only a brief description is given here. Ammonia ions are prepared vibrational state selectively with (2 + 1) resonance-enhanced multiphoton ionization<sup>16</sup> (REMPI) of ammonia in a pulsed molecular beam. This scheme is used to prepare ammonia ions with 0 or 1 quanta in the  $\nu_1$  symmetric stretching (“breathing”) mode and 0–10 quanta of vibrational energy in the  $\nu_2$  symmetric bending (“umbrella”) mode.<sup>17,18</sup> A particular vibrational preparation is described as  $1^m 2^n$  for  $m$  quanta in the  $\nu_1$  mode and  $n$  quanta in the  $\nu_2$  mode. The ions are extracted orthogonally from the molecular beam and injected into a quadrupole mass filter that passes only ions with a mass-to-charge ratio of the desired reactant ion. The reactant ion beam then passes through a collimating lens and into an octopole ion guide<sup>19</sup> in which the reactive collisions occur. The presence of the ion guide ensures the collection of all products, regardless of scattering angle.<sup>14</sup> The neutral collision gas ( $\text{D}_2\text{O}$ , Aldrich, >99.99%) is introduced through a leak valve and into a short collision cell that is concentric with the octopole ion guide. To ensure single-collision conditions, the branching ratios for the various products were measured over a broad collision cell pressure range (roughly 18–60  $\mu\text{Torr}$ ) and were found to be independent of pressure. The reaction collisional energy is experimentally controlled by changing the dc float voltage of the octopole ion guide. The voltage of the field-free ionization region is kept constant at 6.00 V. Changing the octopole dc float voltage over the range 5.08–12.50 V corresponds to a

center-of-mass collisional energy range 0.50–10.00 eV. The product ions and remaining reactant ions drift through the octopole and are mass-selected with a second quadrupole. The time-of-flight profiles for reactants and products are then recorded simultaneously with a multichannel scaler and a current transient recorder.

We report relative integral cross sections that are calculated by normalizing the counted signal for the product in question to the integrated current of the reactant ion. Here “relative” refers to the fact that we are unable to measure absolute cross sections because we know neither the pressure in the collision cell nor the effective path length. Although the units are arbitrary, all of the cross sections reported in the present work may be compared with each other, as the pressure in the collision cell was kept constant for all the experiments (assuming that the conductance between the leak valve and the cell remained constant).

Signal coming from sources other than reactions in the collision cell was checked at all collisional energies by repeating the experiment without introducing D<sub>2</sub>O into the reaction chamber. These background cross sections were found to be the highest for species having a mass-to-charge ratio of 18 but were insignificant even in this case. We suspect this background to be from reaction either with ambient D<sub>2</sub>O in the chamber to form NH<sub>2</sub>D<sup>+</sup> or a hydrogen abstraction reaction from hydrocarbon species in the chamber to form NH<sub>4</sub><sup>+</sup>. The time-of-flight profiles were corrected for collisions outside the collision cell by acquiring data with gas flowing directly into the chamber (not into the collision cell). These background time-of-flight profiles were subtracted from the reactive time-of-flight profiles before the velocity transformation (see below).

Because the reactant ions are generated with a pulsed laser ( $\approx 10$  ns) and ions are measured with a fast detector, the time taken by the reactants and products to traverse the length of the instrument can also be measured. These time-of-flight profiles can then be transformed into the velocity domain if the instrument function is sufficiently well-known. The instrument function is estimated by simulating the guided-ion beam to determine the correlation between ion flight time and ion velocity in the octopole. The accuracy of this lookup table is tested by comparing two different reactant time-of-flight profiles recorded under conditions in which all conditions were held constant except the float voltage of the octopole. This calibration is performed in every experiment for which time-of-flight data are recorded.

Owing to the nature of the octopole ion guide, only the projection of the product velocity onto the instrument axis can be known. The instrument axis is approximately parallel to the velocity of the center of mass ( $\mathbf{v}_{\text{cm}}$ ) because the fast ammonia ion beam collides with a thermal sample of D<sub>2</sub>O vapor. The average speed of the D<sub>2</sub>O molecules is small compared to the speed of the ammonia ion. Therefore, while we cannot determine the degree to which the products of a reaction side scatter, we can accurately determine whether the products are forward- or backward-scattered in the center-of-mass frame.

## Results and Discussion

**Observed Products.** Because product detection is accomplished with a quadrupole mass filter and a charged particle detector, only ionic products are observed. Conservation of charge dictates that any reaction channel will have at least one positively charged product. The major products of the reaction of ammonia ions with deuterated water under the experimental conditions discussed above (single collision,  $E_{\text{cm}} = 0.50$ –10

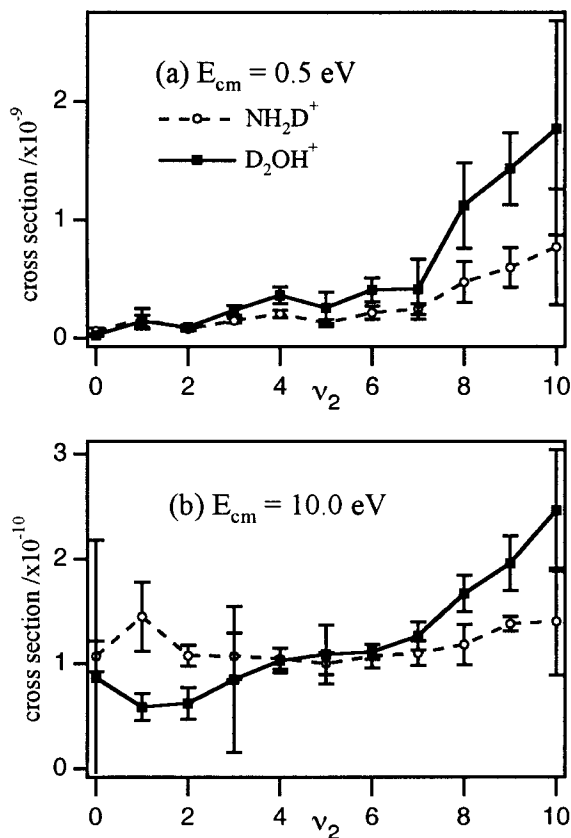


**Figure 1.** Vibrational energy dependence of the reaction of NH<sub>3</sub><sup>+</sup>(1<sup>2n</sup>) with D<sub>2</sub>O to form D<sub>2</sub>OH<sup>+</sup> and NH<sub>2</sub>D<sup>+</sup> at (a) 0.5 and (b) 10.0 eV collisional energy (com). The ordinate is the relative reactive cross section for the reaction forming each channel (arbitrary units). The abscissa is number of quanta of excitation in the  $\nu_2$  normal mode of the ammonia ion (vibrational spacing 0.12 eV).

eV,  $\nu_2 = 0$ –10) have mass-to-charge ratios of 18 and 21 amu. These products are assigned to be NH<sub>2</sub>D<sup>+</sup> (“formal isotope exchange”) and D<sub>2</sub>OH<sup>+</sup> (“proton transfer”), respectively. These assignments are based on several different sources of information: the masses of the major products for other isotopic variations of the reaction (ND<sub>3</sub><sup>+</sup> + H<sub>2</sub>O, ND<sub>3</sub><sup>+</sup> + D<sub>2</sub>O, and NH<sub>3</sub><sup>+</sup> + H<sub>2</sub>O), energetic constraints, and product scattering. There are also small amounts of product with mass-to-charge ratios of 19, 20, and 22; however, they are below the intensity level at which our instrument ceases to be trustworthy. That there is little product at mass 20, one unit less than a major product, attests to the purity of our D<sub>2</sub>O sample. A significant HOD or H<sub>2</sub>O impurity would have yielded product at masses 20 and 19, respectively.

**D<sub>2</sub>OH<sup>+</sup>.** The formation of D<sub>2</sub>OH<sup>+</sup> is enhanced with increasing ammonia ion vibrational energy and yet is inhibited with increasing collisional energy as can be seen in Figures 1 and 2. This behavior could be attributed to the fact that all of the energy in internal modes of the reactants is available to the collision complex, while only part of the collisional energy may be available to the system. For example, if the impact parameter is large (a justifiable assumption in light of the scattering information presented below), the centrifugal barrier will consume increasing amounts of collisional energy. These data could also be taken as evidence in favor of a late barrier along the reaction coordinate, in which case translational energy would be expected to be much less effective than internal energy in enhancing reactivity. Although several models might be put forward, we are reluctant to make strong claims.



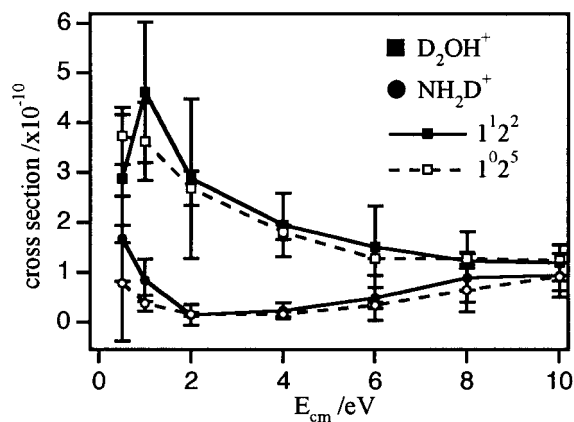


**Figure 2.** Collisional energy dependence of the reaction of  $\text{NH}_3^+(1^1_2^2)$  and  $\text{NH}_3^+(1^0_2^5)$  with  $\text{D}_2\text{O}$  to form  $\text{D}_2\text{OH}^+$  and  $\text{NH}_2\text{D}^+$ . The ordinate is the relative reactive cross section for the reaction forming each channel (arbitrary units).

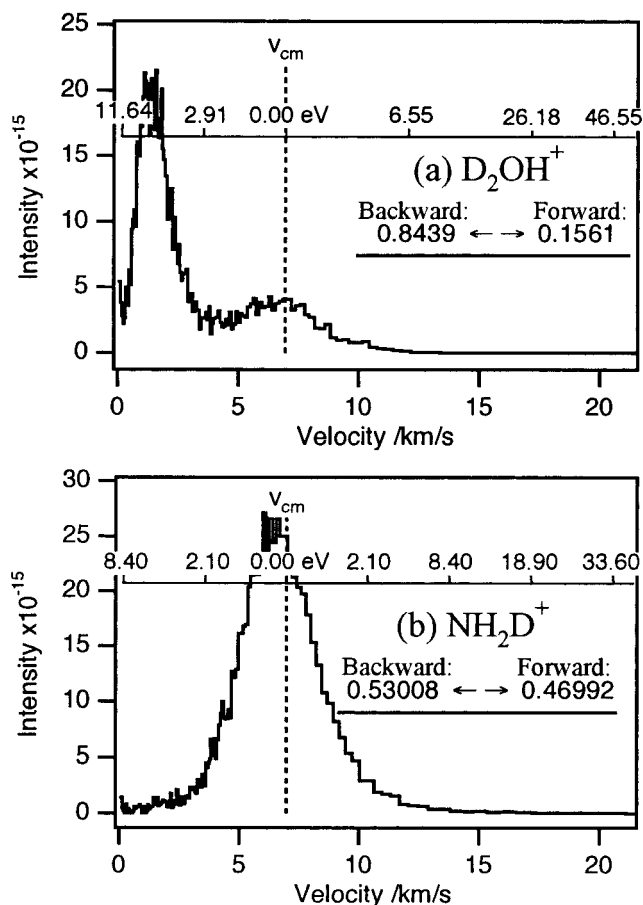
Figure 2 includes the reactivities of two nearly isoenergetic vibrational preparations of  $\text{NH}_3^+$ :  $\text{NH}_3^+(1^1_2^2)$  and  $\text{NH}_3^+(1^0_2^5)$  ( $E_{\text{int}} = 0.63$  and  $0.60$ , respectively). A simple prediction of mode-selective behavior based on motion along the reaction coordinate might be that proton transfer would be enhanced with increasing energy in the  $\nu_1$  symmetric stretching mode. However, no measurable difference exists in reactivity between the two isoenergetic vibrational preparations at any of the collisional energies investigated. This behavior indicates either that  $\text{D}_2\text{OH}^+$  results from a complex that lasts long enough to randomize internal energy or that the effect is too small to be observed in the present experiment.

Figure 3a shows a sample velocity distribution for the reaction of  $\text{NH}_3^+(1^0_2^1)$  with  $\text{D}_2\text{O}$  to form  $\text{D}_2\text{OH}^+$  at a center-of-mass collisional energy of 10 eV. The distribution is bimodal with one peak on the center of mass and one strongly backward-scattered peak. (The forward direction is defined by the initial direction of travel of the reactant ion.) Figure 4 shows how the velocity distribution changes with collisional energy and with ammonia ion vibrational state.

The scattering of this product is consistent with the predictions of the spectator-stripping model<sup>1</sup> in which the velocity of the  $\text{NH}_2$  fragment, the spectator, is assumed not to change throughout the reactive event. The predicted velocity of the  $\text{D}_2\text{OH}^+$  product is readily calculated using this assumption according to the following equation:

$$w_{\text{D}_2\text{OH}^+} = - \frac{m_{\text{NH}_2}}{m_{\text{D}_2\text{OH}^+}} \left( \frac{2E_{\text{cm}} m_{\text{D}_2\text{OH}^+}}{M m_{\text{NH}_3^+}} \right)^{1/2}$$

where  $w_{\text{D}_2\text{OH}^+}$  is the velocity of  $\text{D}_2\text{OH}^+$  in the center of mass frame,  $E_{\text{cm}}$  is the center-of-mass collisional energy,  $M$  is the total mass of the system, and  $m_A$  is the mass of species A. To obtain the lab-frame velocity, these center-of-mass velocities are added to the velocity of the center of mass. This prediction is indicated in Figure 4 by " $v_{\text{SS}}$ ". The experimentally measured velocities of the  $\text{D}_2\text{OH}^+$  product are slightly faster (in the lab frame) than the predictions of the spectator-stripping model. This behavior indicates that the  $\text{NH}_2$  fragment may have lost a small amount of momentum during the reactive event. The agreement with the spectator-stripping model is the worst at the lowest collisional energy studied (0.5 eV, com) where all the available energy is needed to overcome the endothermicity of the reaction and cannot therefore go into scattering of the



**Figure 3.** Velocity distribution for (a)  $\text{D}_2\text{OH}^+$  and (b)  $\text{NH}_2\text{D}^+$  from the reaction of  $\text{NH}_3^+(1^0_2^1)$  with  $\text{D}_2\text{O}$  at 10 eV collisional energy. The abscissa is the lab frame velocity of the product in the octopole after reaction. The floating scale is the total center-of-mass energy in product recoil.

products. A second possible cause for the slight disagreement with the spectator-stripping model is that the slowest ions would be susceptible to perturbation by nonideal electric fields in the instrument. For example, heating could be caused by imperfections in the trapping field of the octopole or fringing fields at the exits and entrances of the various rf devices. Also note that off-axis scattering (a deviation from true spectator-stripping behavior) would tend to make the axial projection of the velocity seem more forward scattered.

The velocity distribution in Figure 3a shows a minor amount ( $\approx 30\%$ ) of product scattering with velocities near that of the center of mass. A careful inspection of the absolute intensities of this peak in Figure 4c (note different vertical scales) seems to indicate that this slower contribution is not enhanced by vibrational energy, unlike the fast backward-scattered peak. Both the scattering along the center of mass and the fact that formation of these products is not enhanced with increased vibrational energy indicate that this contribution could be caused by formation of a complex, similar to that for  $\text{NH}_2\text{D}^+$ , described in detail below.

**$\text{NH}_2\text{D}^+$ .** The elucidation of the dynamics leading to the formation of  $\text{NH}_2\text{D}^+$  is not as straightforward. This channel shows several curious features. First, its relative cross section (Figure 2) shows two distinct collisional energy trends—falling at low collisional energy and rising again starting at  $\approx 5$  eV (com). Second, although up to 10 eV of energy is available to the system in the form of kinetic energy of the reactants, very little energy goes into product recoil. This conclusion is clearly

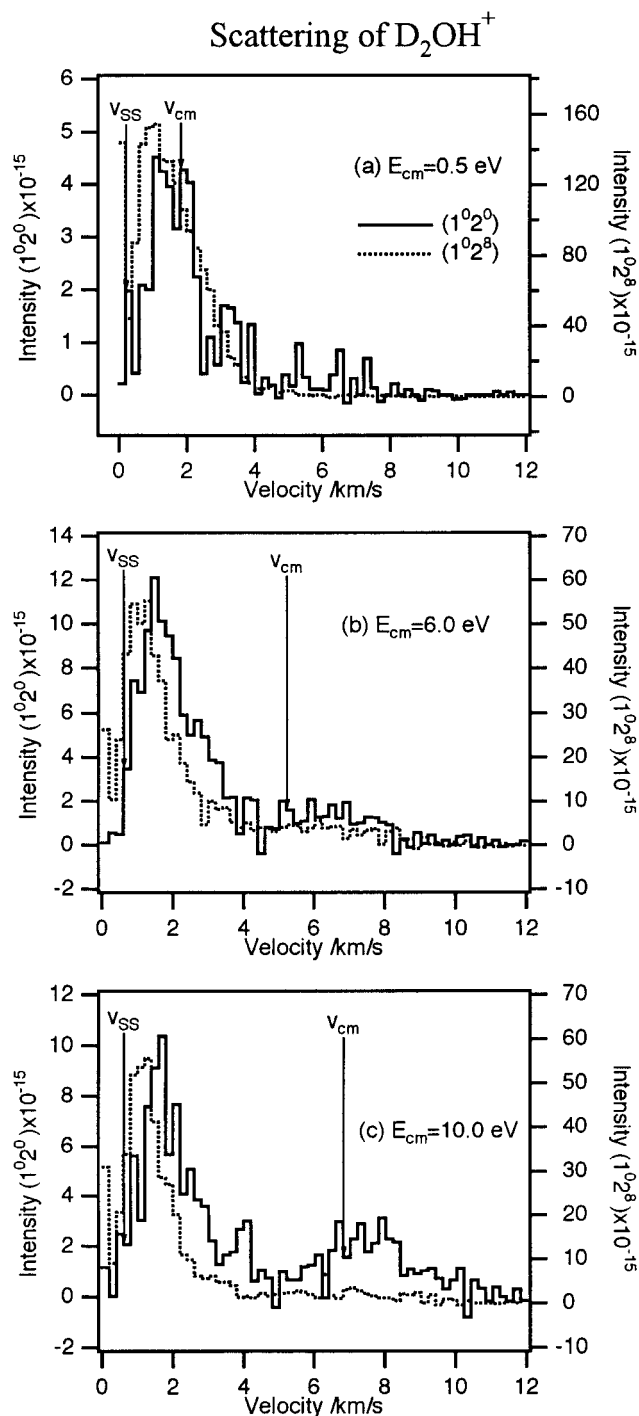


**Figure 4.** Velocity distributions for  $\text{D}_2\text{OH}^+$  from the reaction of  $\text{NH}_3^+(1^{020})$  (solid lines, left-hand axis) and  $\text{NH}_3^+(1^{028})$  (dashed lines, right-hand axis) with  $\text{D}_2\text{O}$  at center-of-mass collisional energies of 0.5, 6.0, and 10 eV. The velocity of the center of mass is indicated with  $v_{\text{cm}}$ . The prediction of the spectator-stripping model is indicated with  $v_{\text{ss}}$ . Note the different scaling for the two curves in each plot.

shown by Figure 3b as the product is seen to scatter tightly to (0.6 eV, hwhm) and symmetrically about (53% faster, 47% slower) the center of mass. Figure 5 demonstrates that this behavior is observed at all collisional energies. Third, a product showing similar collisional energy dependence and product scattering has been observed<sup>20</sup> for the reactions of  $\text{NH}_3^+$  with  $\text{D}_2$  and  $\text{CD}_4$ —both of these reactions turning on at roughly 5 eV (com) and depositing very little energy into product recoil. Fourth, practically no product was observed at mass 19 at any of the collisional energies studied. If the  $\text{NH}_2\text{D}^+$  were formed

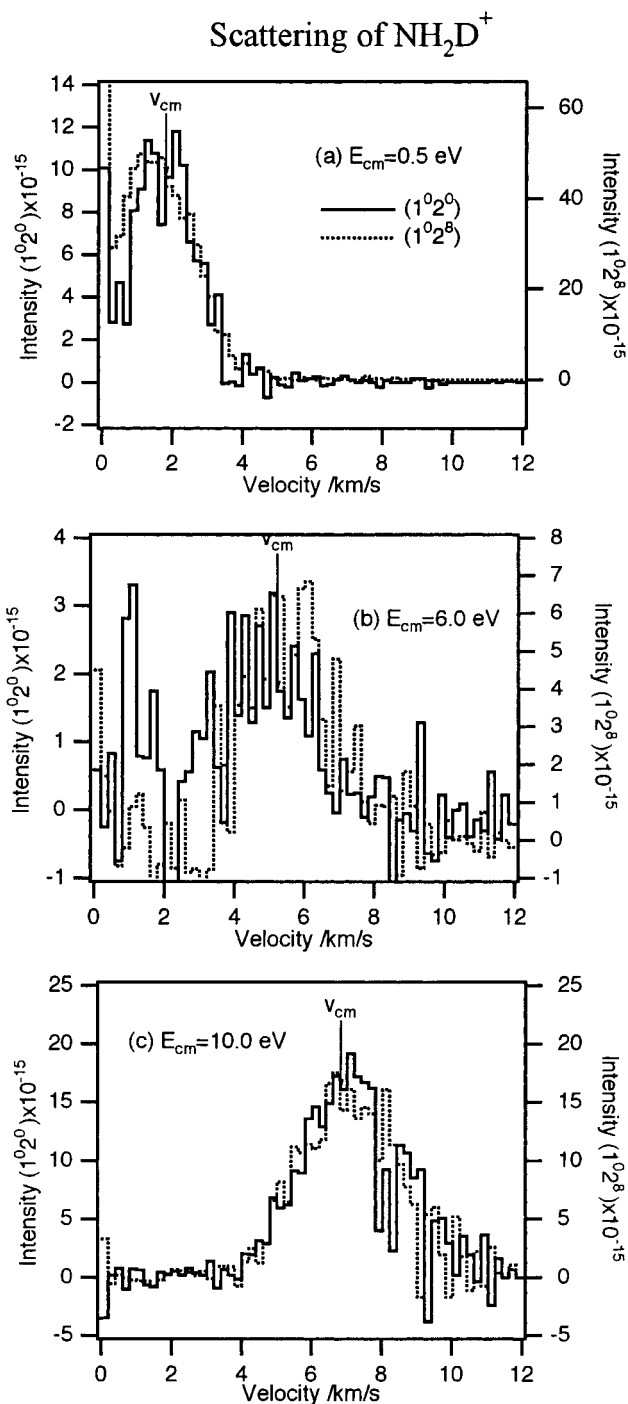


**Figure 5.** Velocity distributions for  $\text{NH}_2\text{D}^+$  from the reaction of  $\text{NH}_3^+(1^{020})$  (solid lines, left-hand axis) and  $\text{NH}_3^+(1^{028})$  (dashed lines, right-hand axis) with  $\text{D}_2\text{O}$  at center-of-mass collisional energies of 0.5, 6.0, and 10 eV. The velocity of the center of mass is indicated with  $v_{\text{cm}}$ . Note the different scaling for the two curves in each plot.

via a direct stripping of a deuterium atom followed by a unimolecular decay, significant amounts of  $\text{NH}_3\text{D}^+$  would be expected to form at collisional energies below the threshold for formation of  $\text{NH}_2\text{D}^+$ . Moreover,  $\text{NH}_2\text{D}^+$  from this mechanism would most likely scatter in the forward direction.

A model that accounts for all of these observations is one in which the  $\text{NH}_2\text{D}^+$  is formed by a two-step mechanism: a collision-induced dissociation-mediated complex formation followed by the dissociation of this complex into products. According to this model, formation of a long-lived complex is contingent on the breakage of either an ammonia N—H bond

or a water O–D bond. After this collision-induced dissociation step, sufficient energy has been lost by bond rupture that the remaining complex ( $[\text{NH}_2\text{D}_2\text{O}]^+$  in the former case or  $[\text{NH}_3\text{-DO}]^+$  in the latter) has a lifetime sufficiently long to transfer one or more of the hydrogen isotopes prior to dissociation. If this description is the true mechanism yielding  $\text{NH}_2\text{D}^+$ , however, these complexes still have short lifetimes, as we are able to detect neither the complexes, themselves, nor see evidence for metastable species in the second quadrupole. We place an upper bound of 20  $\mu\text{s}$  on the lifetime of the complex.

With sufficiently high collisional-energy resolution it may be possible to differentiate between these two pathways (N–H bond breakage vs O–D bond breakage), but this task is currently beyond the scope of the present experiment. A second way to differentiate between these two channels would be to detect the neutral product with a technique such as laser-induced fluorescence. The  $[\text{NH}_2\text{D}_2\text{O}]^+$  complex would dissociate forming OD whereas the  $[\text{NH}_3\text{DO}]^+$  complex would yield OH. The product fluxes in the present experiment (on the order of one product every few seconds) are too low to permit this kind of measurement. That we also observe a small amount of  $\text{D}_2\text{OH}^+$  scattering at the center-of-mass velocity supports the conclusion that  $\text{NH}_2\text{D}^+$  is formed via a  $[\text{NH}_2\text{D}_2\text{O}]^+$  complex.

### Conclusions

The reaction of vibrationally state-selected ammonia ions with deuterated water molecules at high collisional energies shows several interesting traits. The major product at thermal energies ( $\text{NH}_3\text{D}^+ + \text{OD}$ ) is barely detectable by our apparatus under the highly energetic conditions (0.5–10 eV) studied. Instead, we observe two different products, one of which has not been previously reported ( $\text{NH}_2\text{D}^+ + \text{OH}(\text{D}) + \text{D}(\text{H})$ ). We propose that the latter is formed through a complex resulting from collision-induced dissociation; this complex then dissociates into the products. Our observations of the second major product,  $\text{D}_2\text{OH}^+$ , are consistent with those predicted by the spectator-stripping model. This reactive system is found not to be sensitive to the specific vibrational preparation of the ammonia ion for the collisional energy range investigated, only to the total internal energy.

The fact that there is no charge-transfer channel observed in this system leads us to speculate that the strong mode selectivity

observed in the isoelectronic reaction of ammonia ions with deuterated ammonia was mainly driven by the large Franck–Condon overlap of the charge-transfer channel. This type of mode selectivity would obtain only for ion–molecule reactions. We suggest that other reactions of ammonia ions that include a direct charge-transfer product might also demonstrate some degree of mode selectivity. Future experiments are being planned to test the hypothesis of Franck–Condon control of mode selectivity in ion–molecule chemistry.

**Acknowledgment.** The authors gratefully acknowledge the financial support of the Air Force Office of Scientific Research (Grant F49620-92-J-0074).

### References and Notes

- (1) Levine, R. D.; Bernstein, R. B. *Molecular Reaction Dynamics and Chemical Reactivity*; Oxford University Press: New York, 1987.
- (2) Mallard, W., Ed. *NIST Chemistry WebBook*; volume 69 NIST: <http://webbook.nist.gov/chemistry>, 1998.
- (3) Chupka, W. A.; Russell, M. E. *J. Chem. Phys.* **1968**, *48*, 1527–1533.
- (4) Anicich, V. G.; Kim, J. K.; Huntress, W. T. *Int. J. Mass Spectrom. Ion Phys.* **1977**, *25*, 433–438.
- (5) Chesnavich, W. J.; Bowers, M. T. *Chem. Phys. Lett.* **1977**, *52*, 179–183.
- (6) Adams, N. G.; Smith, D.; Paulson, J. F. *J. Chem. Phys.* **1980**, *72*, 288–297.
- (7) Kemper, P. R.; Bowers, M. T.; Parent, D. C. *J. Chem. Phys.* **1983**, *79*, 160–169.
- (8) Tachibana, A.; Kawauchi, S.; Nakamura, K.; Inaba, H. *Int. J. Quantum Chem.* **1996**, *57*, 673–682.
- (9) Green, R. J.; Zare, R. N. *J. Chem. Phys.* **1997**, *107*, 772–778.
- (10) Zare, R. N. *Science* **1998**, *279*, 1875–1879.
- (11) Guettler, R. D.; Jones, Jr., G. C.; Posey, L. A.; Zare, R. N. *Science* **1994**, *266*, 259–261.
- (12) Chiu, Y.; Fu, H.; Huang, J.; Anderson, S. L. *J. Chem. Phys.* **1995**, *102*, 1199–1216.
- (13) Fu, H.; Qian, J.; Green, R. J.; Anderson, S. L. *J. Chem. Phys.* **1998**, *108*, 2395–2407.
- (14) Guettler, R. D.; Jones, Jr., G. C.; Posey, L. A.; Kirchner, N. J.; Keller, B. A.; Zare, R. N. *J. Chem. Phys.* **1994**, *101*, 3763–3771.
- (15) Posey, L. A.; Guettler, R. D.; Kirchner, N. J.; Zare, R. N. *J. Chem. Phys.* **1994**, *101*, 3772–3786.
- (16) Anderson, S. L. *Adv. Chem. Phys.* **1992**, *82*, 177–212.
- (17) Miller, P. J.; Colson, S. D.; Chupka, W. A. *Chem. Phys. Lett.* **1988**, *145*, 183–187.
- (18) Conaway, W. E.; Morrison, R. J. S.; Zare, R. N. *Chem. Phys. Lett.* **1985**, *113*, 429–434.
- (19) Gerlich, D. *Adv. Chem. Phys.* **1992**, *82*, 1–176.
- (20) Unpublished results.